



Supplement of

Measurement report: Insights into the chemical composition and origin of molecular clusters and potential precursor molecules present in the free troposphere over the southern Indian Ocean: observations from the Maïdo Observatory (2150 m a.s.l., Réunion)

Romain Salignat et al.

Correspondence to: Clémence Rose (c.rose@opgc.fr)

The copyright of individual parts of the supplement might differ from the article licence.

S1. Models

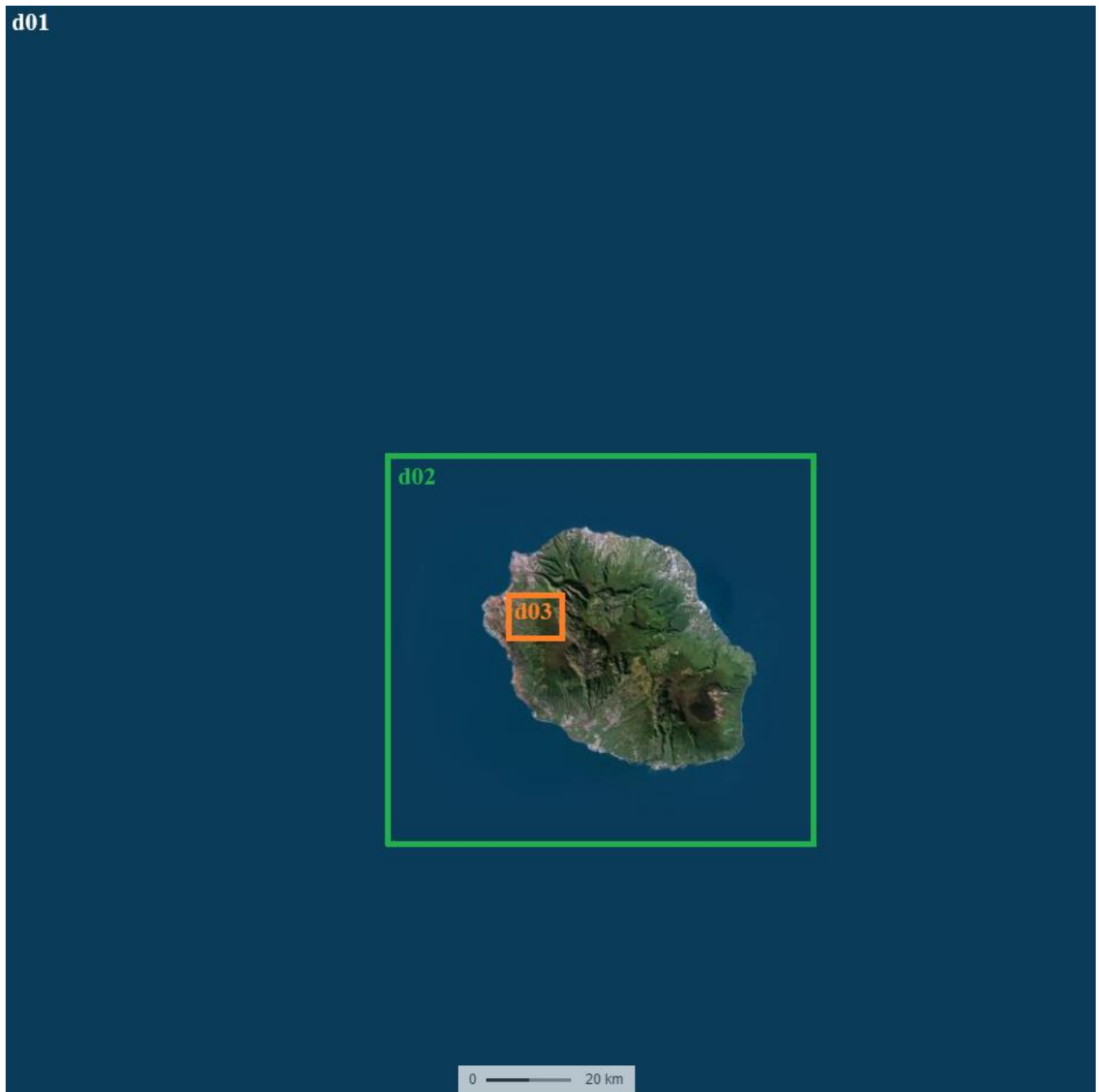


Figure S1 The extent of Meso-NH's three domains with horizontal resolution of 2000 (d01), 500 (d02) and 100 m (d03). The map was obtained from <https://www.geoportail.gouv.fr/> (last access: February 02, 2024).

S2. Identification of a tracer of free tropospheric conditions

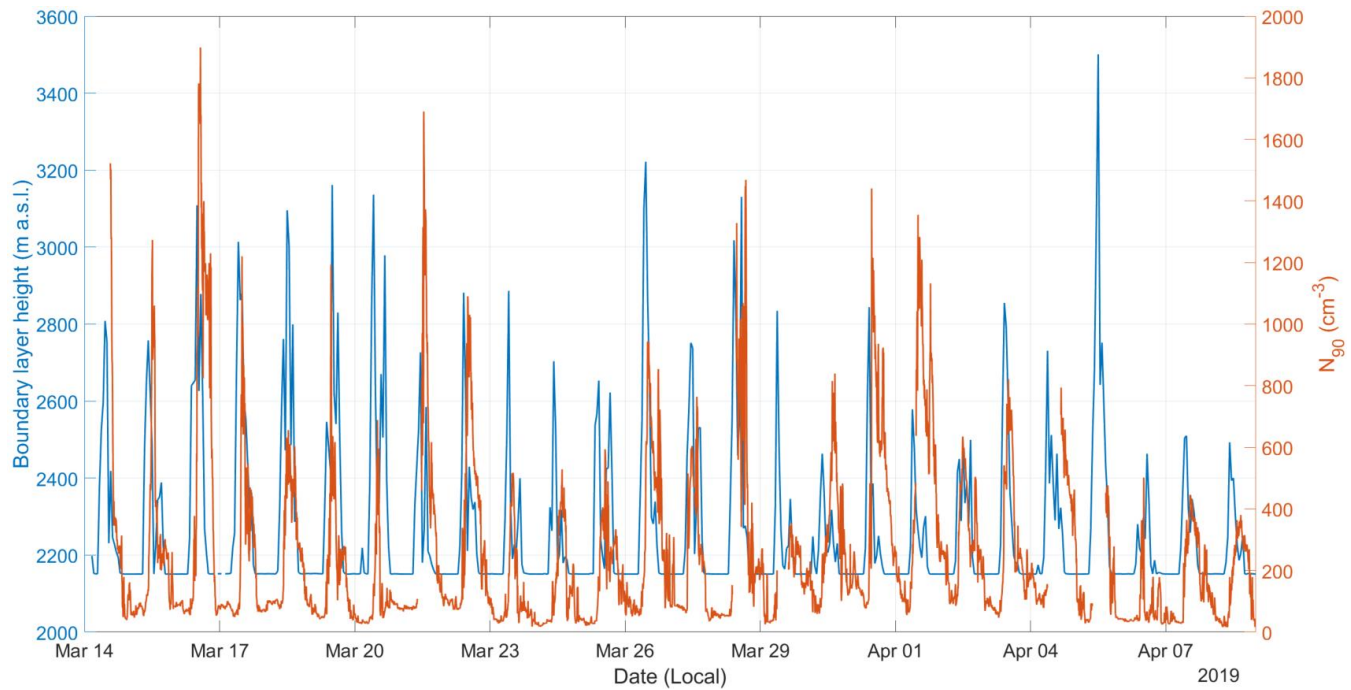


Figure S2 Time series of the BLH simulated by Meso-NH for the model grid point which includes the Maïdo observatory in the innermost domain (blue) and number concentration of particles > 90 nm (N_{90}) measured at the site (red).

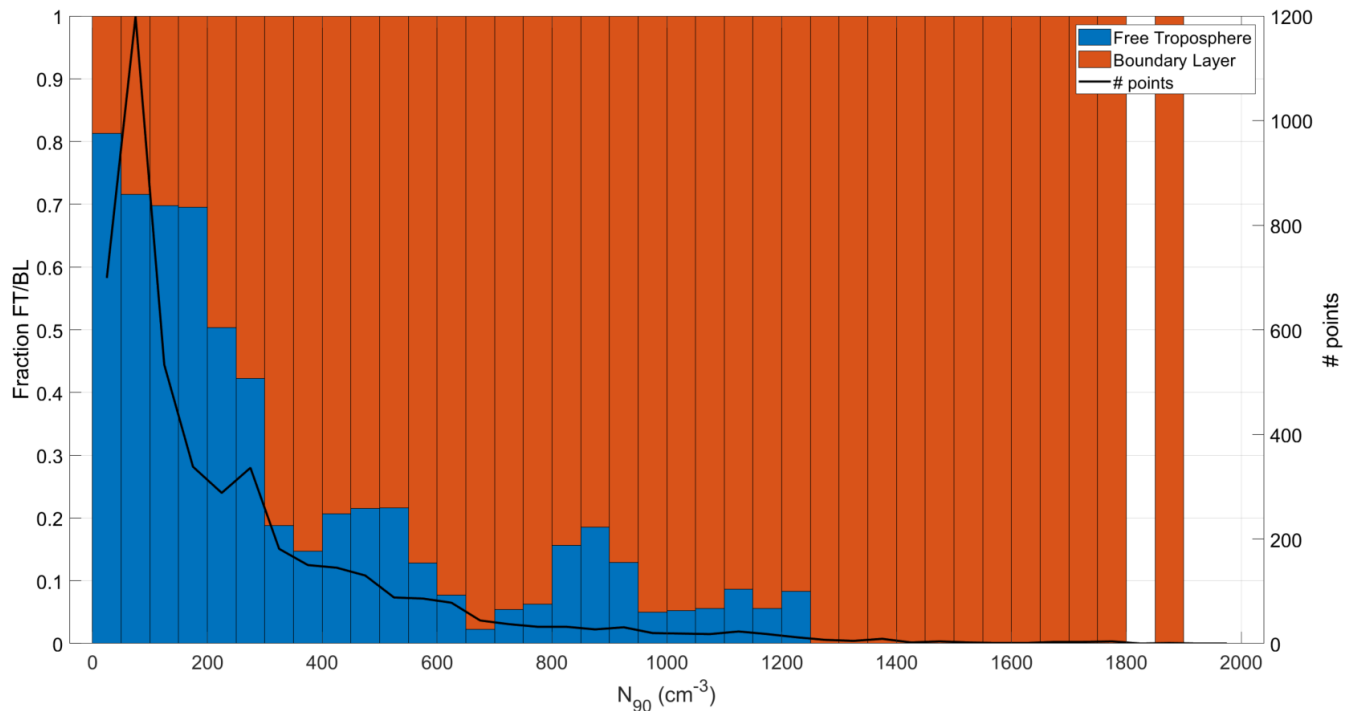


Figure S3 Number concentration of particles > 90 nm (N_{90}) segregated between FT and BL conditions at Maïdo. The percentage of hours for which Meso-NH indicates that the station is in the BL or in the FT for each N_{90} bin (50 cm^{-3} width) is shown on the y-left-axis. The number of points in each bin is represented on the y-right-axis to provide further information on the distribution of the data.

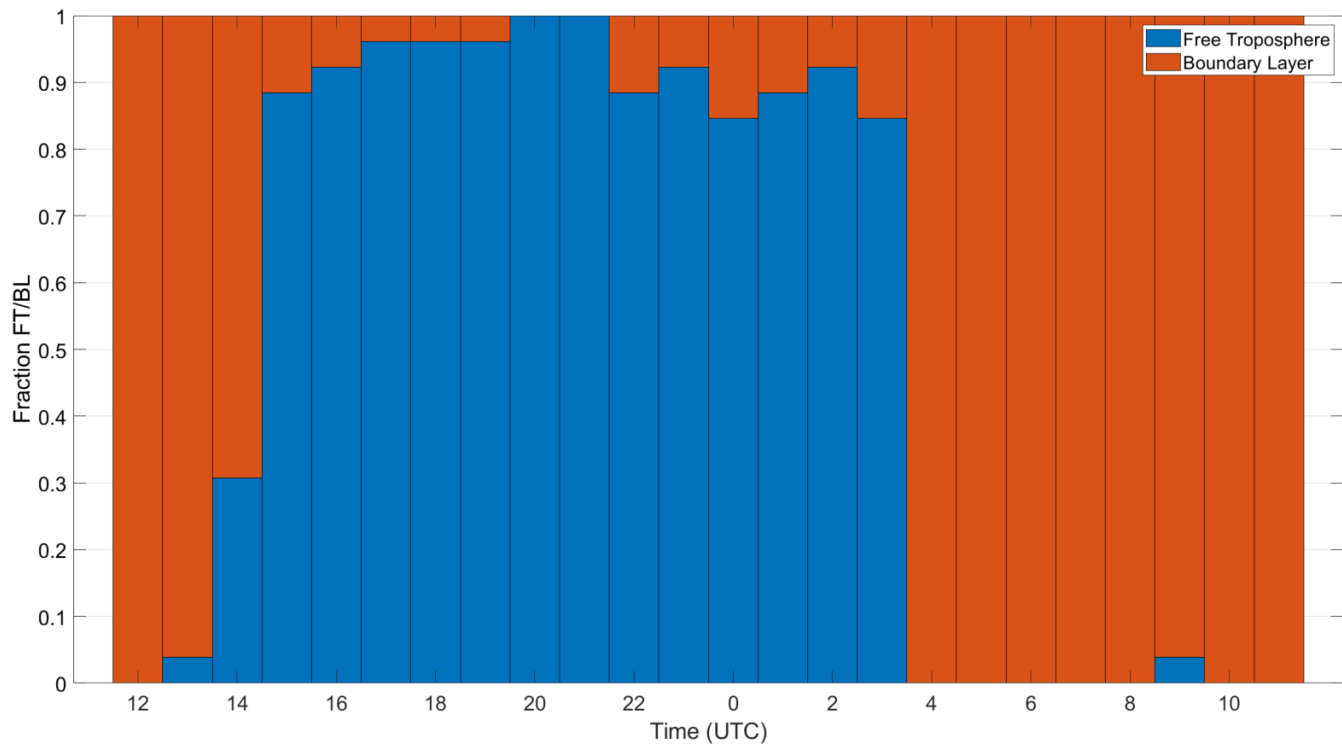


Figure S4 Percentage of data for which Meso-NH indicates that the station is in the BL or in the FT for each hour of the day. For each hour, the reported statistics are based on 26 model outputs.

5

10

15

S3. Positioning of the air masses in the FT or in the BL during the hours preceding their arrival at the site

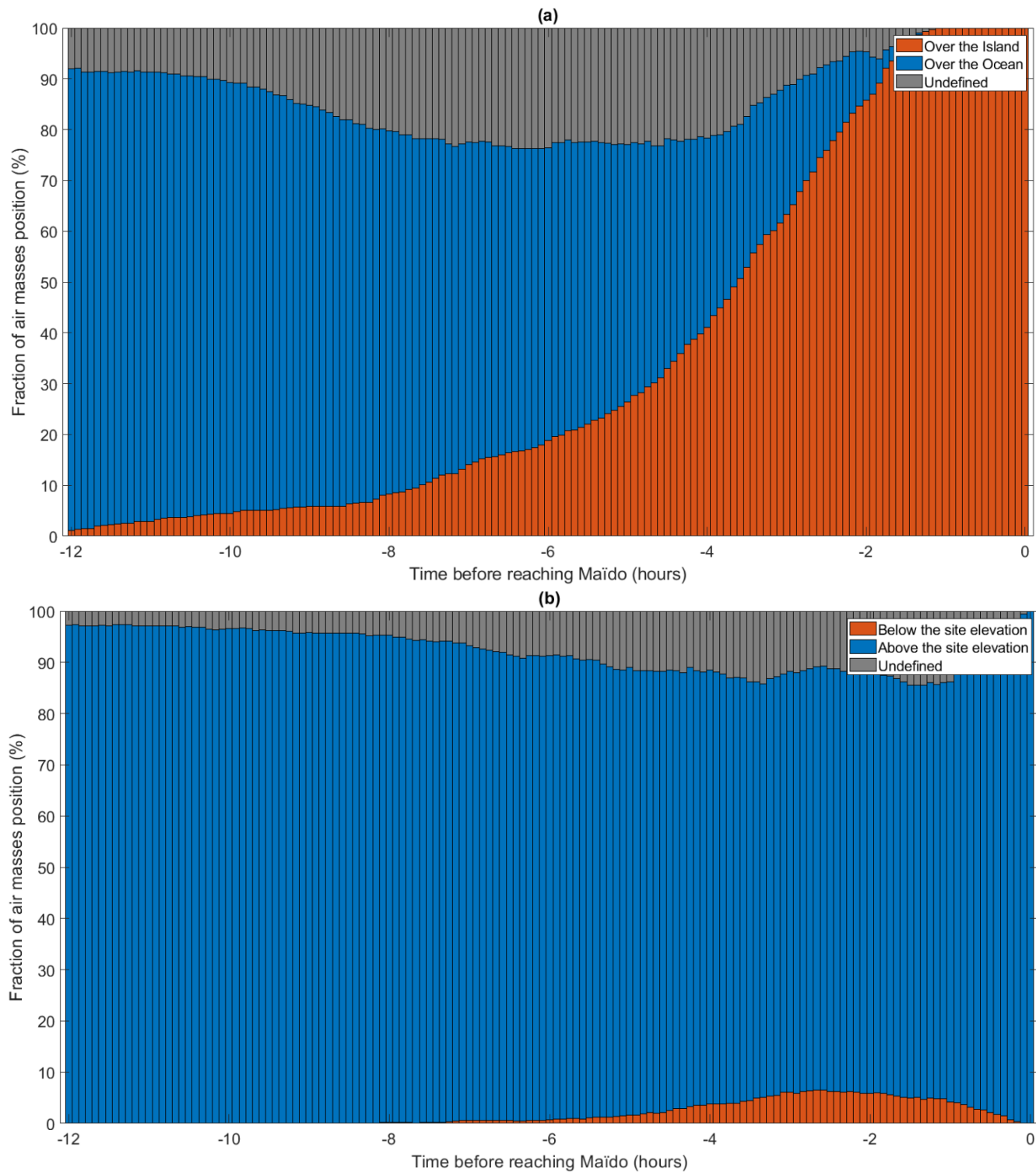


Figure S5 Position of the air masses arriving at Maïdo in the FT along their path a. over land or ocean and b. relative to the site elevation. Twelve hours back-trajectories were computed with Meso-CAT during BIO-MAIDO and for each of the back-trajectory points along their path, air masses were considered to be over land or over the ocean (or below/above the station elevation) if 75% of the 324 trajectories in the trajectory set were over land or over the ocean (or below/above the station elevation). Otherwise, their positioning was classified as undefined.

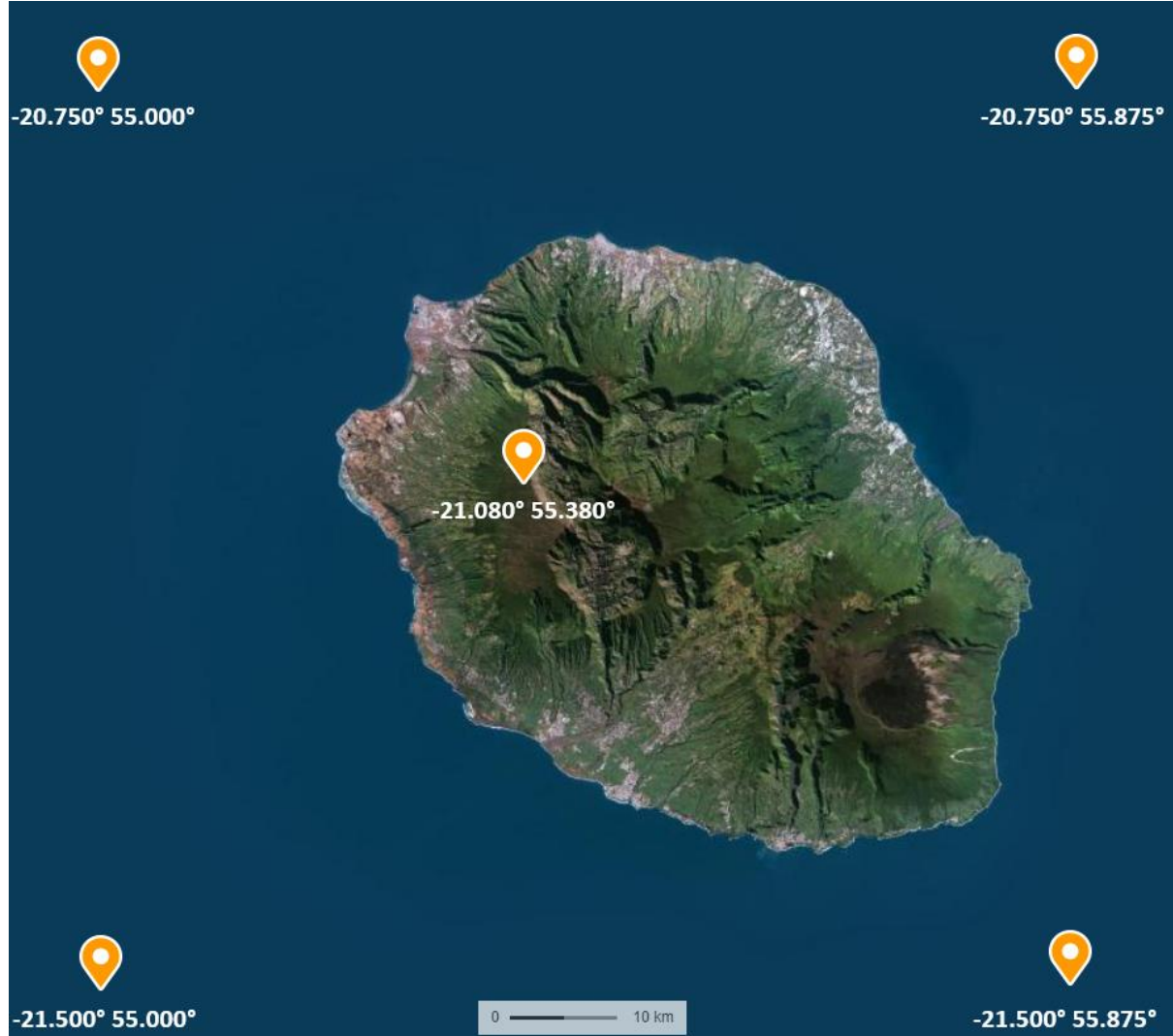
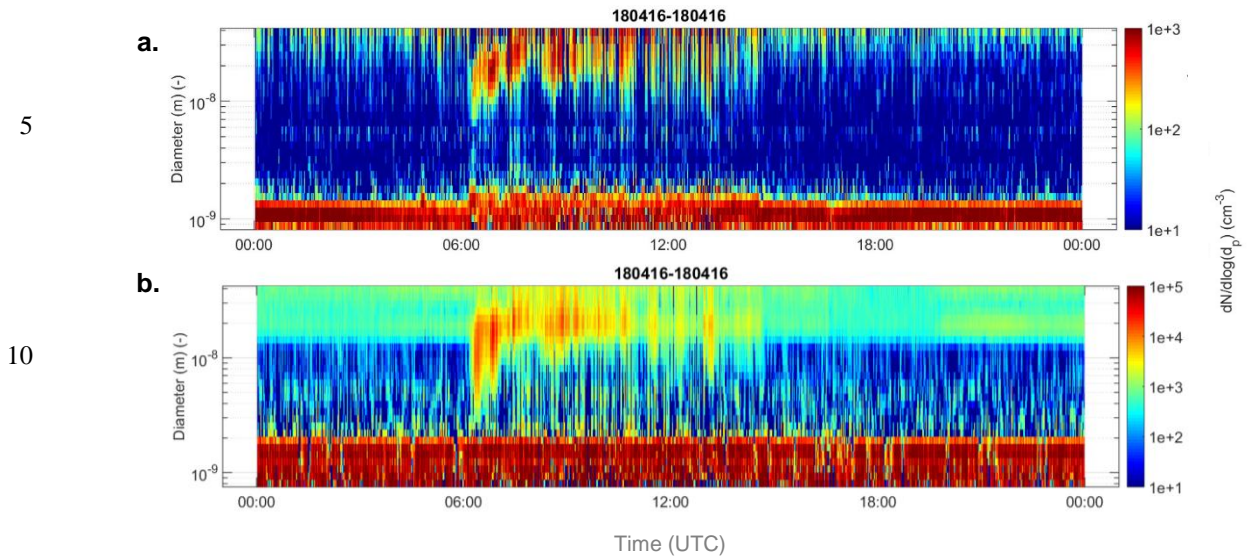


Figure S6 Positioning of the locations used in the sensitivity study performed to assess the reliability of the BL thicknesses retrieved by ECMWF ERA-5 reanalyses. The map was obtained from <https://www.geoportail.gouv.fr/> (last access: June 16, 10 2023).

S4. Overview of the conditions during the OCTAVE campaign



15 Fig. S7 Diurnal variation of a. negative ion and b. particle number size distribution measured with a NAIS on April 16th, 2018.

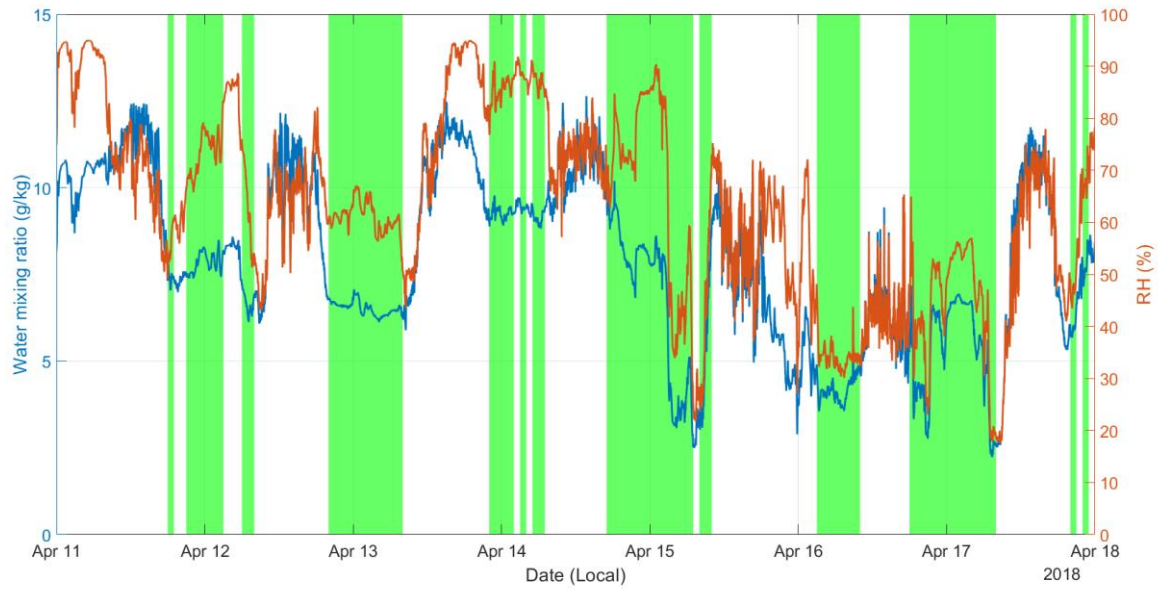


Fig. S8 Timeseries of the water mixing ratio (blue) and relative humidity (RH, orange) during the OCTAVE campaign. Green patches depict the hours when the Maido station is in the FT based on the analysis of the standard deviation of the horizontal wind direction.
20

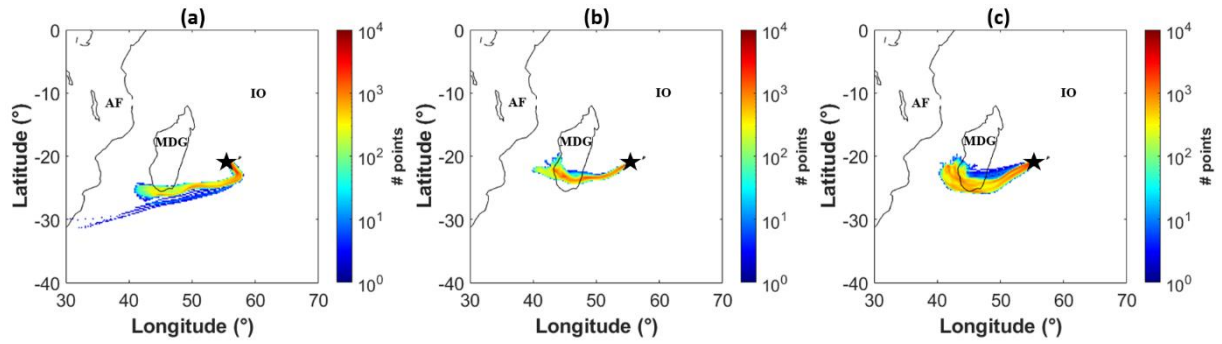
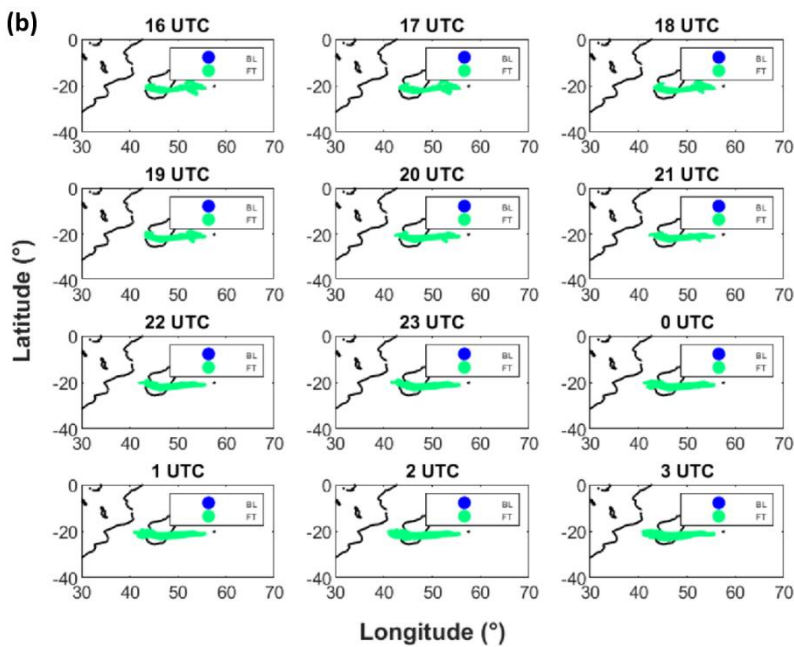
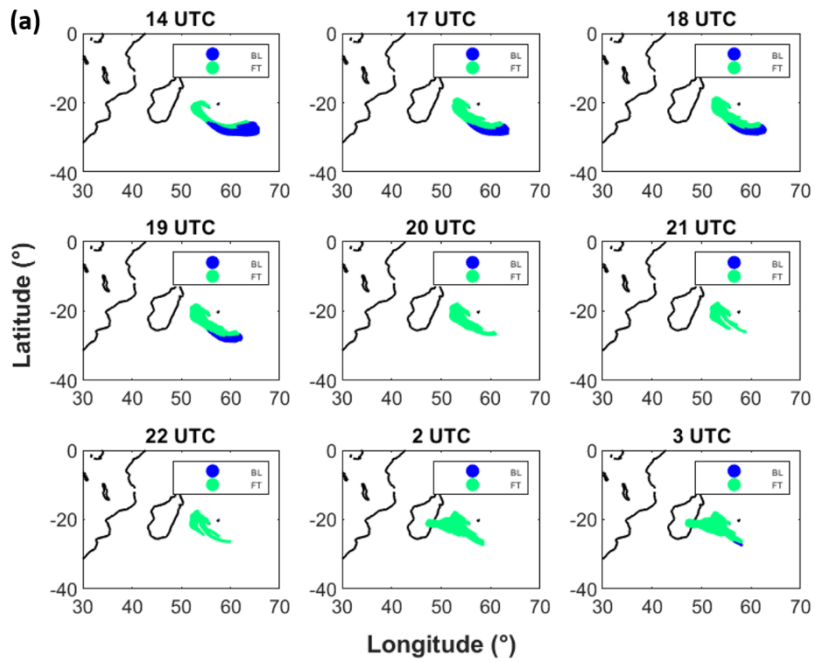
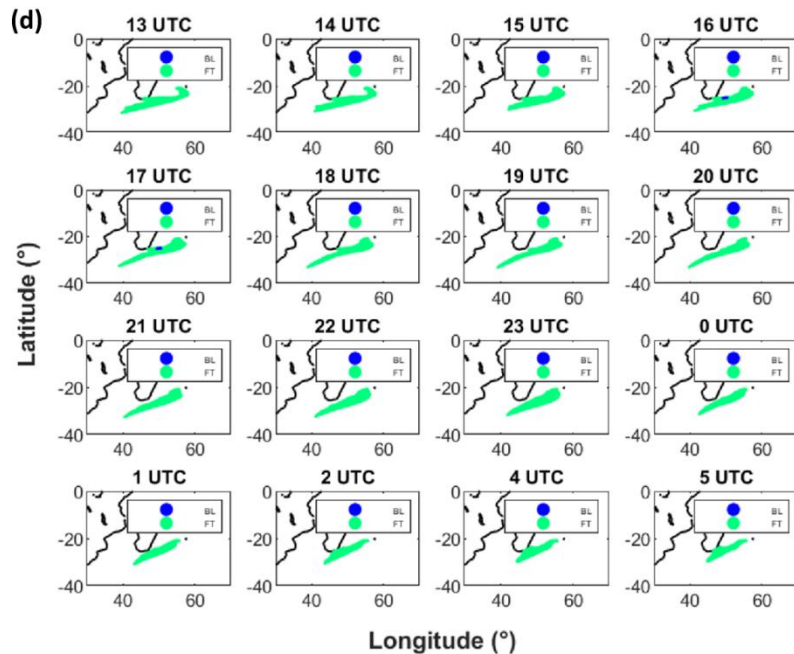
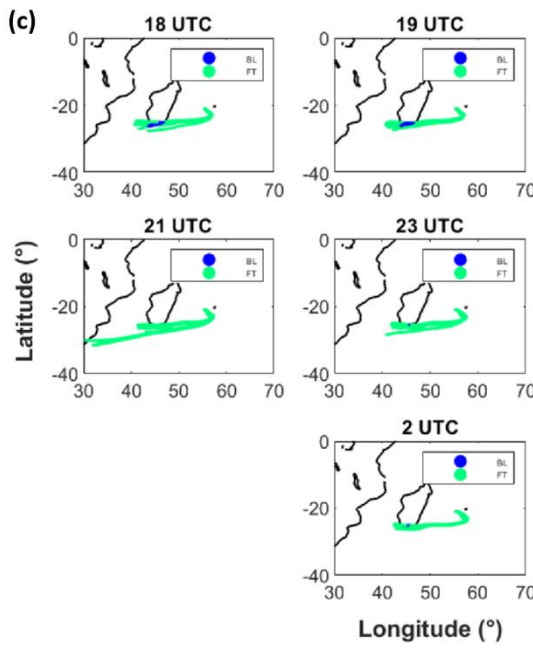


Figure S9 72-hour back-trajectories of the air masses arriving at Maïdo (marked by the black star on the maps) when the station
 5 was in FT conditions during the nights of April a. 13 to 14, b. 15 to 16 and c. 16 to 17, 2018. The colour of each grid cell
 (0.2x0.2°) on the maps indicates the number of back-trajectory points falling into its area. Note that for each back-trajectory
 computed with the CAT model, all 125 trajectories of the corresponding set are shown in the figure. The abbreviations AF,
 MDG and IO stand for Africa, Madagascar, and Indian Ocean, respectively.

10

15





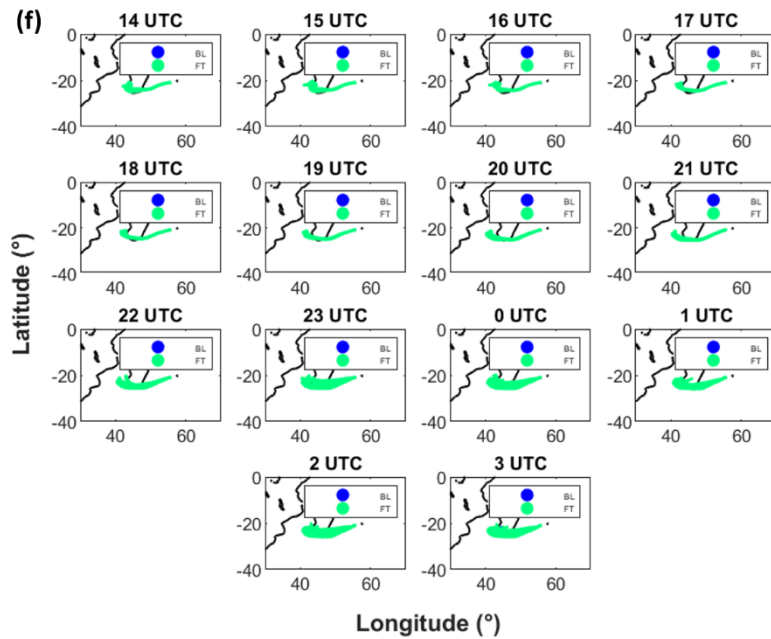
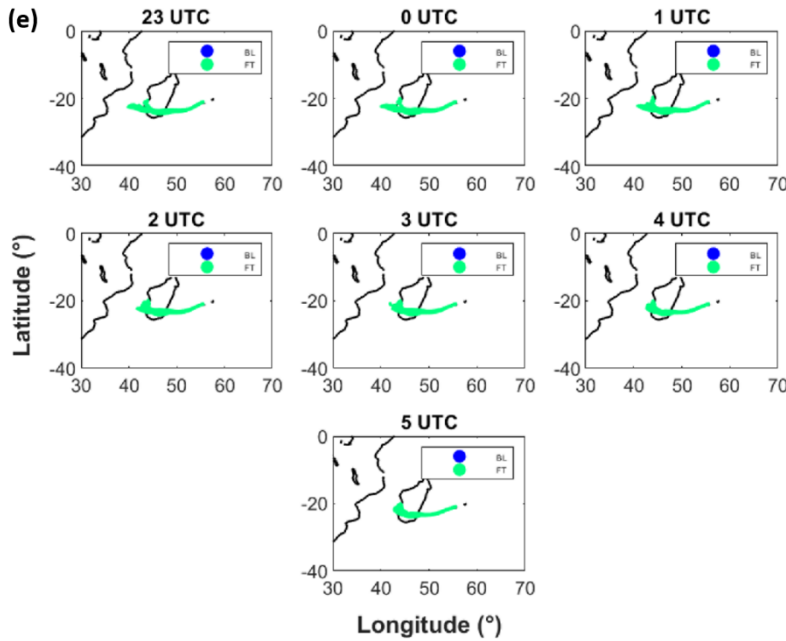


Figure S10 Positioning of air masses (in the FT or in the BL, as indicated by CAT) arriving in the FT at Maïdo along their 72-hour back-trajectory during the nights of April a. 11 to 12, b. 12 to 13, c. 13 to 14, d. 14 to 15, e. 15 to 16 and f. 16 to 17, 2018.

5 Note that for each back trajectory computed with the CAT model, all 125 trajectories of the corresponding set are shown in the figure.

S5. Insights into the chemical composition of molecular clusters and their precursors in the marine FT

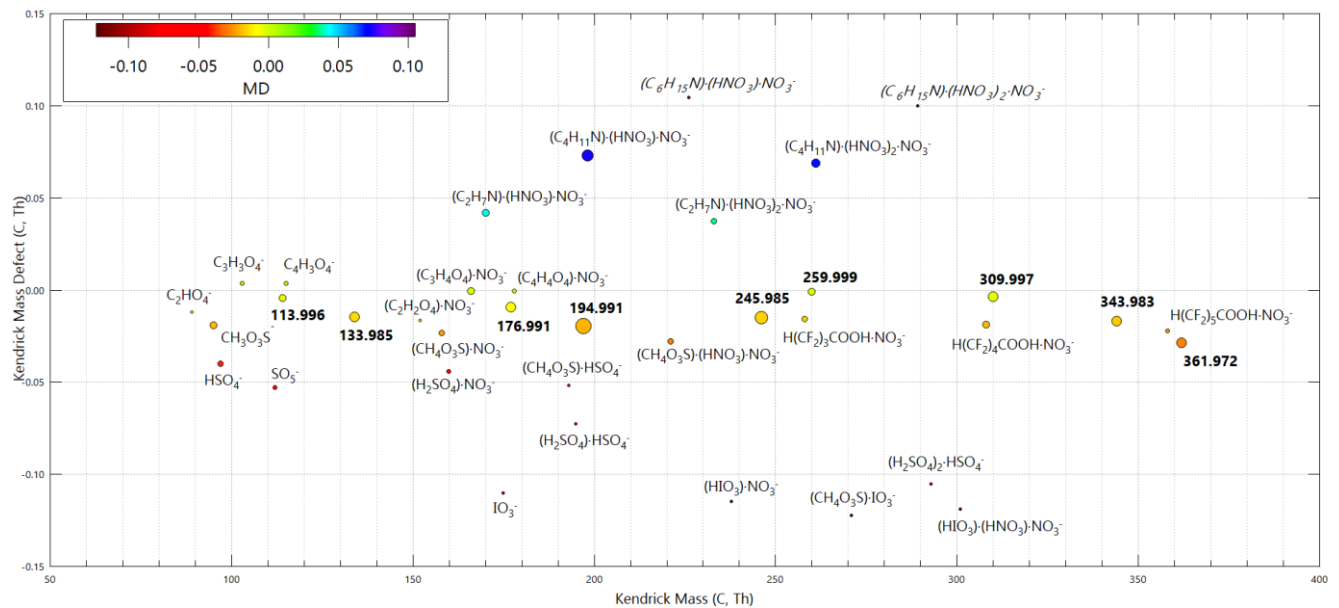


Figure S11 Mass defect plot (corresponding to the data shown in Fig. 6.a) showing the identified species (marked by their chemical composition) as well as non-identified compounds associated to major peaks in the spectrum (marked by their mass, 5 in bold). The size of the markers is related to the signal intensity (logarithmic scale).

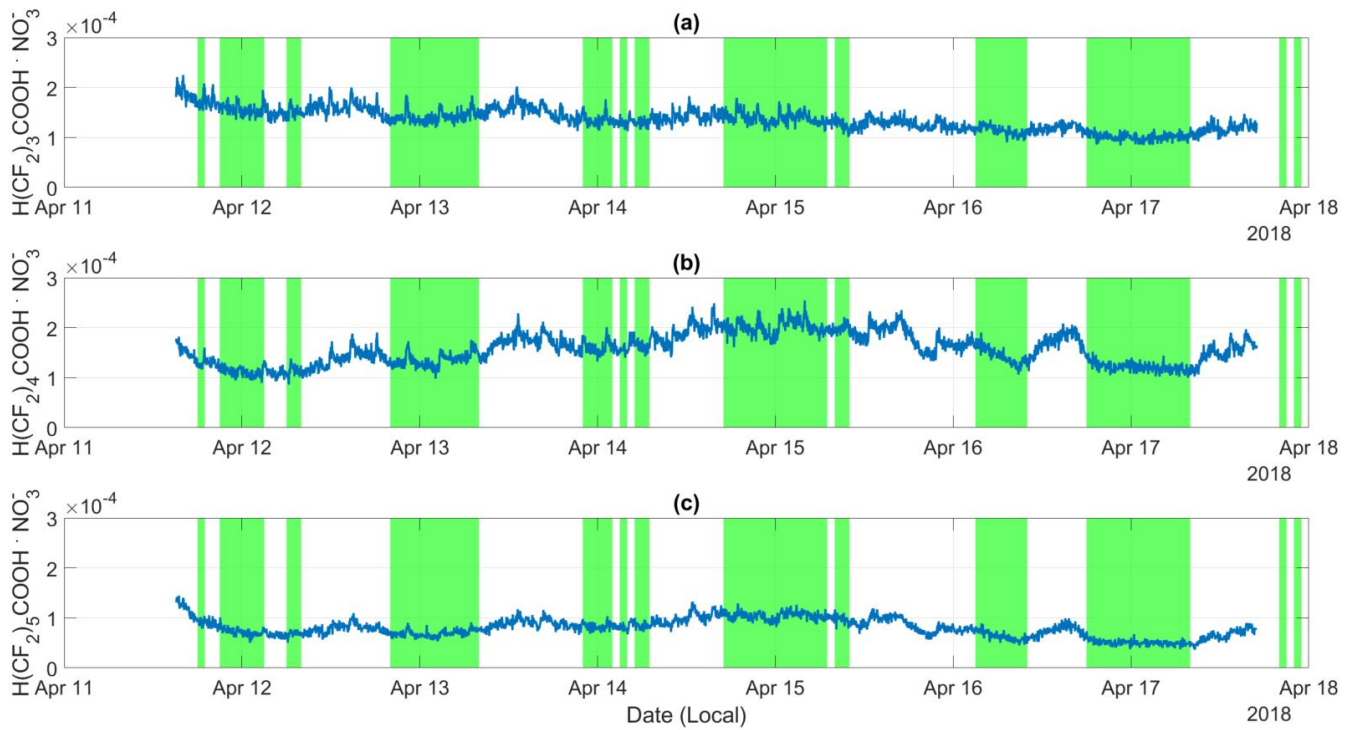


Figure S12 Time series of the fluorinated compounds normalized signal a. $H(CF_2)_3COOH \cdot NO_3^-$, b. $H(CF_2)_4COOH \cdot NO_3^-$ and c. $H(CF_2)_5COOH \cdot NO_3^-$. Green patches depict the hours when the Maido station is in the FT based on the analysis of the standard deviation of the horizontal wind direction.

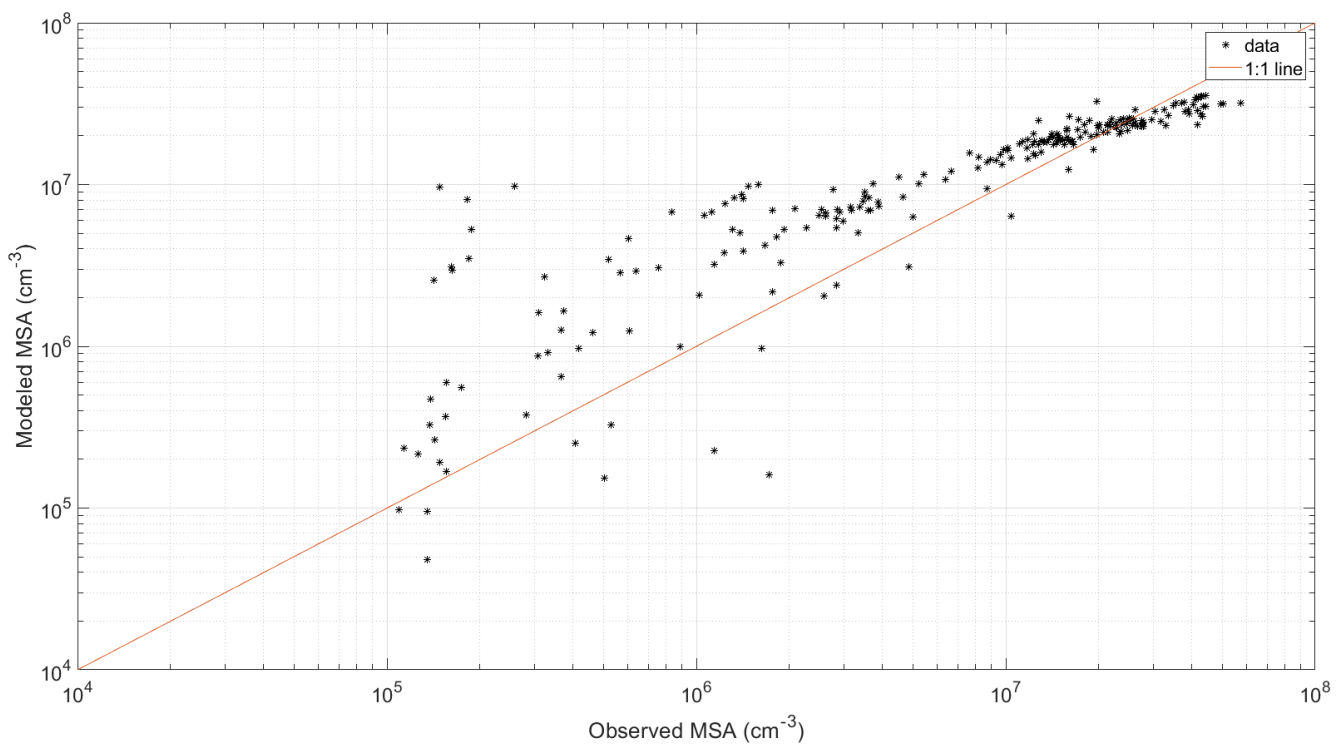


Figure S13 Scatter plot illustrating the close match between the results of the linear regression model determined from fitting RH and CS data to MSA concentrations measured in the FT ($MSA = -5.63 \times 10^5 \times RH + -1.97 \times 10^{10} \times CS + 5.20 \times 10^7$, referred to as *Modeled MSA*) and measured MSA concentrations.

5

10

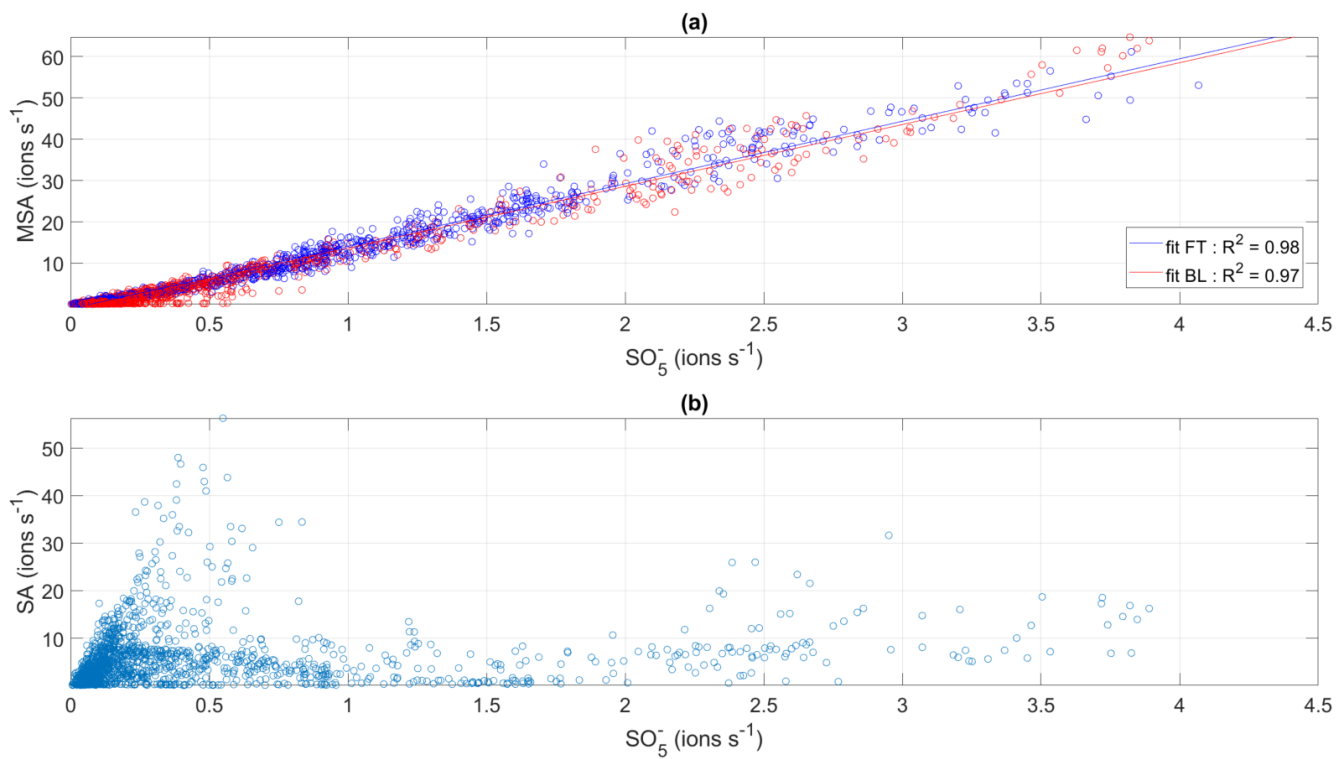


Figure S14 Correlations of SO_5^- with a. MSA, separately in the BL and in the FT and with b. sulfuric acid during daytime (i.e. when global radiation $> 10 \text{ W m}^{-2}$).

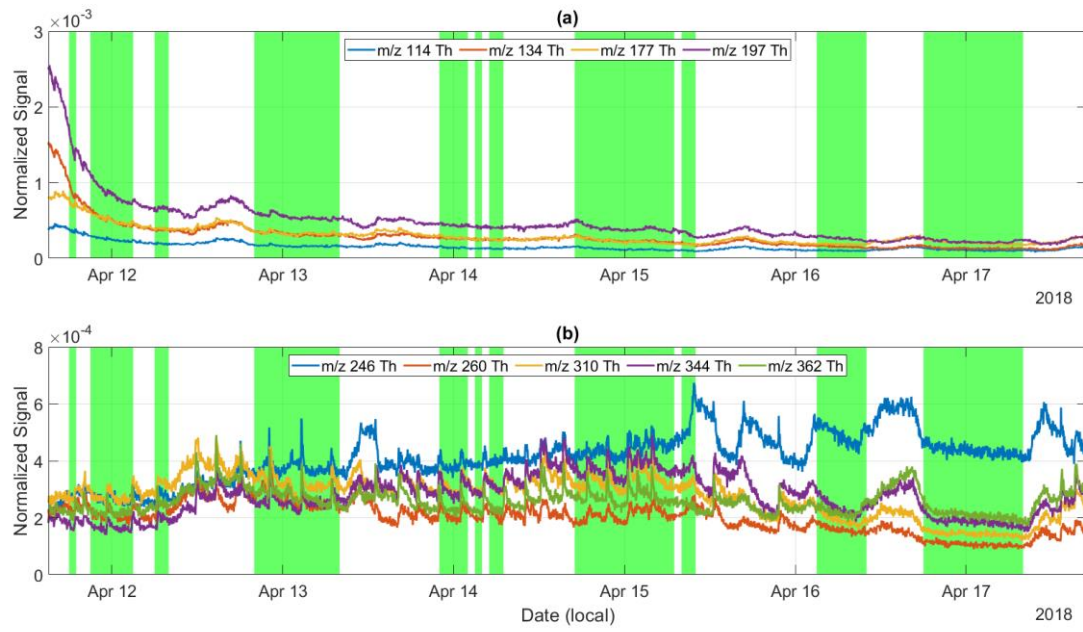


Figure S15 Timeseries of the normalized signals of UMR a. 114, 134, 177 and 197 Th and b. 246, 260, 310, 344 and 362 Th. Green patches depict the hours when the Maïdo station is in the FT based on the analysis of the standard deviation of the horizontal wind direction.

5

10

15

20

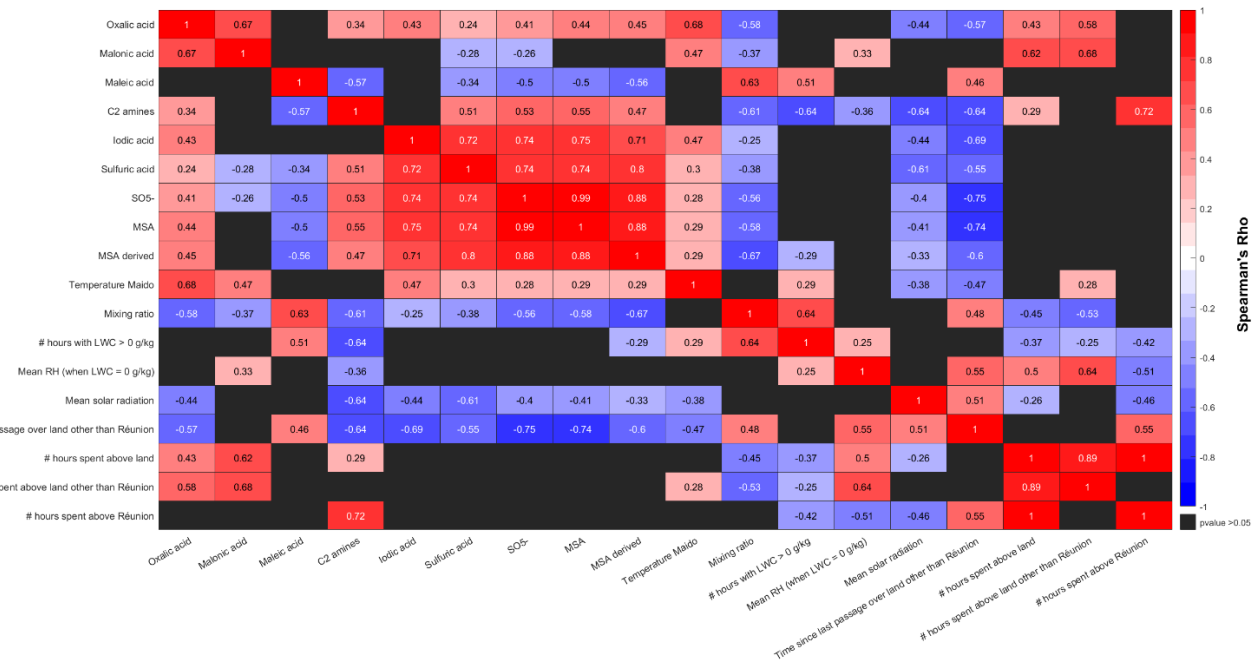


Figure S16 Similar to Fig. 10 in the main text, with in addition inter-species and inter-parameter correlations.

Table S1 Monoterpene oxidation products used as fingerprint molecules for the study of HOMs sources in the boreal forest by Yan et al. (2016).

Compound	UMR (Th)
$C_{10}H_{14}O_7\cdot NO_3^-$	308
$C_{10}H_{15}O_8\cdot NO_3^-$	325
$C_{10}H_{15}O_5NO_3\cdot NO_3^-$	339
$C_{10}H_{14}O_9\cdot NO_3^-$	340
$C_{10}H_{15}O_6NO_3\cdot NO_3^-$	355
$C_{10}H_{15}O_{10}\cdot NO_3^-$	357
$C_{10}H_{15}O_8NO_3\cdot NO_3^-$	387
$C_{20}H_{32}O_{11}\cdot NO_3^-$	510
$C_{20}H_{31}O_8NO_3\cdot NO_3^-$	523
$C_{20}H_{32}O_6(NO_3)_2\cdot NO_3^-$	554
$C_{20}H_{31}O_{10}NO_3\cdot NO_3^-$	555